Quaternary Science Reviews 221 (2019) 105862

Contents lists available at ScienceDirect

Quaternary Science Reviews

journal homepage: www.elsevier.com/locate/quascirev

Tracing the last remnants of the Scandinavian Ice Sheet: Ice-dammed lakes and a catastrophic outburst flood in northern Sweden

Carl Regnéll*, Jan Mangerud, John Inge Svendsen

Department of Earth Science, University of Bergen, PO Box 7803, NO-5020, Bjerknes Centre for Climate Research, Bergen, Norway

ARTICLE INFO

Article history:
Received 27 May 2019
Received in revised form
24 July 2019
Accepted 31 July 2019
Available online xxx

Keywords:
Quaternary
Glaciation
Scandinavia
Geomorphology
Glacial
Deglaciation
IDL
GLOF
Fennoscandian ice sheet
Early Holocene
Isostasy

ABSTRACT

We present geomorphological evidence of large, previously undocumented, early Holocene ice-dammed lakes in the Scandinavian Mountains of northwestern Sweden. The lakes extents indicate that the last remnants of the Scandinavian Ice Sheet were located east of the mountain range. Some early pioneering works have presented similar reconstructions, whereas more recently published reconstructions place the last ice remnants in the high mountains of Sarek.

Using high-resolution airborne LiDAR data we have mapped a large number of hitherto undocumented shorelines in some of the main valleys within the northern Scandinavian mountain range. Our results indicate that a larger system of ice-dammed lakes existed in this region than previously thought. The lakes were dammed between the main water divide to the west and the retreating ice sheet margin to the east. The shorelines dip towards the northwest with gradients ranging from 0.5 to 0.4 m/km, from the oldest to the youngest. Further, we have compiled Lateglacial and Holocene shoreline data along the Norwegian coast and from within the Baltic Sea basin and reconstructed the isostatic uplift along a 1400 km long northwest-southeast transect from the Norwegian Sea to Lake Ladoga. By comparing the measured ice-dammed lake shoreline gradients to the dated marine shorelines, we infer that the lakes may have existed for several centuries following 10.2 cal ka BP. We also describe large deposits and extensive erosive features, which demonstrate that a catastrophic glacial lake outburst flood (GLOF) took place eastward along the Pite River Valley. Based on cross-cutting relations to raised shorelines developed in the early Holocene Ancylus Lake (Baltic Sea basin) we conclude that the flood and thus the final phase of deglaciation took place within the time interval 10.3–9.9 cal ka BP.

1. Introduction

Distinct shorelines, located high above present-day lakes and valley floors, were described from the central Scandinavian mountain range already in 1734 CE by Carl von Linné (Linnæus, 1734). By the late 19th and early 20th century many more such shorelines had been found all along the mountain range and was interpreted to have been formed along ice-dammed lakes occupying valleys where glacier ice blocked the drainage at the end of the last Ice Age (e.g. Hansen, 1886; Svenonius, 1886; Högbom, 1892; Gavelin and Högbom, 1910; Holmsen, 1915). Possibly the best known example of such a lake is the early Holocene, 1500–1600 km^2 and 100 km^3 large, glacial lake Nedre Glomsjø in Mid-Norway and its subsequent catastrophic drainage (e.g. Hansen, 1886; Holmsen, 1915; Longva, 1994; Høgaas and Longva, 2016, 2018). In northern Scandinavia, large systems of ice-dammed lakes were believed to have formed between the main water divide in the west and an eastward retreating ice sheet margin that blocked the drainage in that direction (e.g. Svenonius, 1885, 1886; Hansen, 1886; Pettersen, 1887; Högbom, 1892). Thus, it was assumed that during deglaciation, the last remnants of the Scandinavian Ice Sheet were located east of the water divide in northern Sweden, that runs north-south within the mountain range along the Swedish-Norwegian border (Fig. 1) (e.g. Svenonius, 1886; Högbom, 1892; Gavelin and Högbom, 1910; Frödin, 1921). In contrast to this, Hoppe (1959) postulated that the ice sheet retreated towards the high mountain areas where it disintegrated into smaller ice-caps centered around the highest mountain massifs in northern Sweden, e.g. Kebnekaise, Sarek and Sulitelma (Fig. 2). Hoppe (1959) based his interpretations on mapped glacial striae, drumlins and glaciofluvial deposits. However, later it was discovered that many of

* Corresponding author.
E-mail addresses: Carl.Regnell@uib.no (C. Regnéll), Jan.Mangerud@uib.no (J. Mangerud), John.Svendsen@uib.no (J.I. Svendsen).

https://doi.org/10.1016/j.quascirev.2019.105862

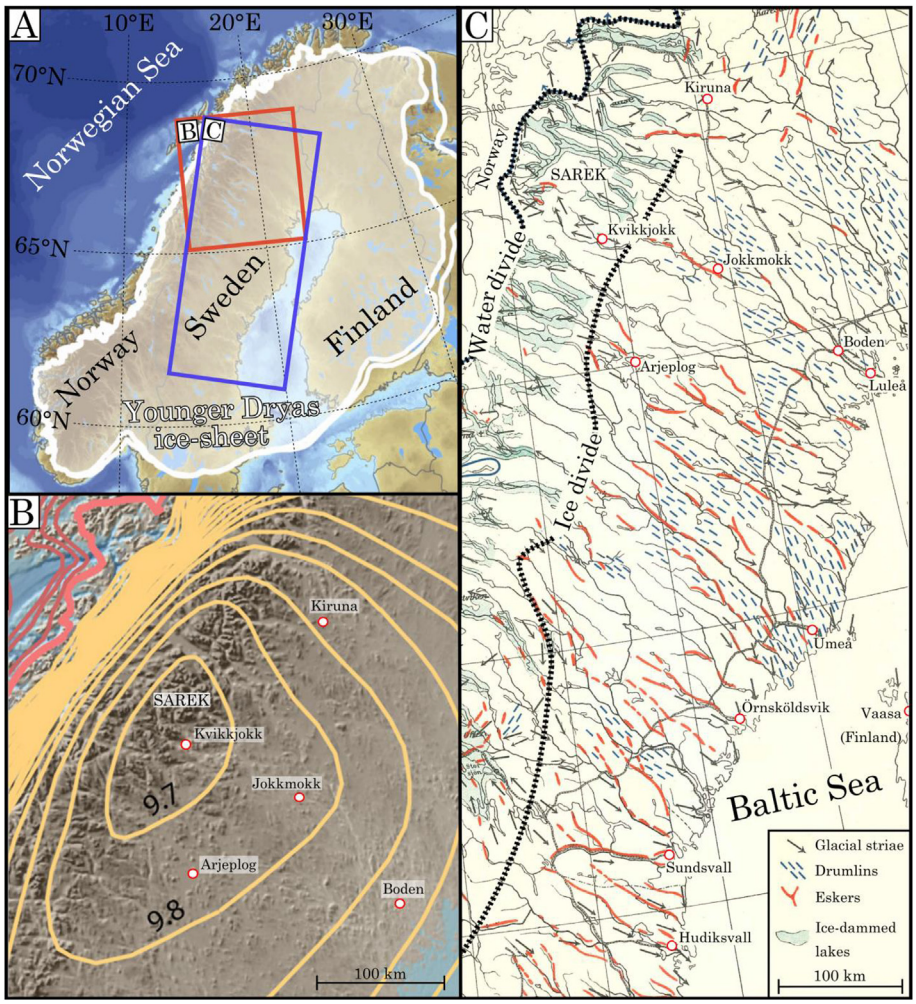

Fig. 1. A. Younger Dryas ice-sheet extent (modified from Hughes et al. 2016) and marked location of Fig. 1B and C. B. Ice-retreat pattern and ages for northern Scandinavia, according to Stroeven et al. (2016). Red lines mark pre-Holocene ice margins and yellow lines Holocene ice margins. C. Glacial geological map of northern Sweden, modified from Gavelin and Högbom (1910). Note the ice-dammed lakes between the water divide and inferred ice divide. (For interpretation of the references to colour in this figure legend, the reader is referred to the Web version of this article.)

these landforms were preserved from older glacial events due to a largely cold-based ice sheet during the final deglaciation (e.g. Lagerbäck, 1988; Rodhe, 1988; Kleman, 1990, 1992). Nevertheless, ice-retreat towards the highest parts of the mountain range is still proposed in several more recent studies (Kleman, 1992; Kleman et al., 1997; Boulton et al., 2001; Stroeven et al., 2016). In the reconstruction of Hughes et al. (2016), on the other hand, the last ice remnant was placed east of the water divide.

The timing of the final deglaciation in this region is poorly constrained and only based on a few basal radiocarbon dates from small lake basins, dating the start of organic sedimentation following deglaciation. The existing dates suggest that the last ice masses melted away prior to 9.5 cal ka BP (e.g. Karlén, 1979; 1981; Rosén et al., 2001). Stroeven et al. (2016) collected all available deglacial dates, including a number of previously published and unpublished terrestrial cosmogenic nuclide dates from northern Sweden. They reconstructed isochrones for the ice front position for every 100-years during deglaciation. Their last isochron (9.7 cal ka BP) was placed around the Sarek Mountains, representing the ice margin just before the ice was supposed to have disappeared completely (Fig. 1C).

In this study, we use the high-resolution airborne LiDAR (Light Detection And Ranging) data set of Sweden. The LiDAR data not only provide the means to map landforms with unprecedented precision, but also led us to discover a number of glacial geological features that had not been described before. Based on these new observations, we reconstruct in detail the ice-dammed lakes and their drainage routes. In turn, we use the lakes to locate the contemporaneous ice sheet margin to the east, i.e. where the ice sheet blocked the drainage. We provide an independent age constraint of the very last phase of deglaciation based on cross-cutting relationships between glacial lake outburst flood (GLOF) landforms and dated early Holocene shorelines from the former Ancylus Lake in the Baltic Sea basin. We also discuss the climatic and dynamic forcing that we suspect determined the course of the final deglaciation.

2. Study area

The study area is located in northern Scandinavian Mountain Range along the main water divide between the Norwegian Sea and the Baltic Sea (Fig. 2). This study also includes the Pite River Valley, which extends further to the east (Fig. 2). In the west the landscape is characterized by high mountains with several peaks reaching above 2000 m a.s.l., dissected by fjords and deep U-valleys with valley floors at around 400–500 m a.s.l. A more gentle terrain

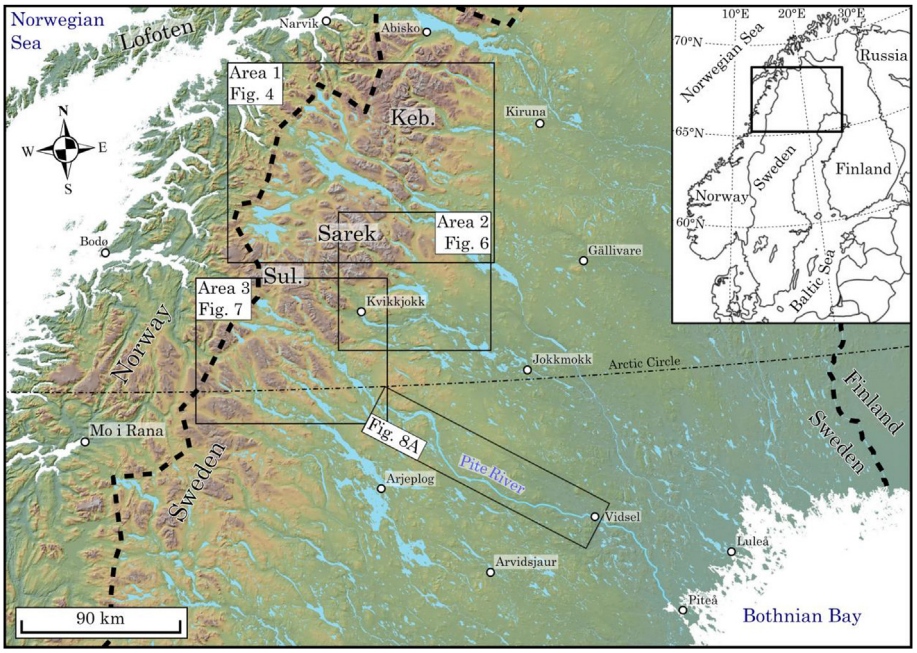

Fig. 2. Overview map of the study areas (Background map: EU-DEM v1.1). Keb. = Kebnekaise mountains, Sul. = Sulitelma mountains.

characterizes the area east of the mountains (Fig. 2). We have mainly studied the area east of the water divide, where all rivers today run to the Baltic Sea. The Pite River, one of the four remaining unregulated large rivers in northern Sweden, flows eastward for more than 400 km from the mountains around Sulitelma to the Bothnian Bay in the northern Baltic Sea (Fig. 2).

3. Methods and materials

The identification and mapping of landforms was performed using aerial images and the Swedish LiDAR based terrain model '*Nationell Höjdmodell*' (National Height model), produced by the Swedish national mapping agency (Lantmäteriet; http://www.lantmateriet.se). The height model has a pixel resolution of 2 m, an average vertical accuracy of ~0.1 m in flat terrain respectively 0.2 m in varied terrain and is delivered pre-processed without vegetation cover (Rönnberg, 2011; Lantmäteriet, 2019). As background map in figures of larger land areas we used the EU-DEM v1.1 terrain model (https://land.copernicus.eu/imagery-in-situ/eu-dem/eu-dem-v1.1/view) which is delivered with a 25 m pixel resolution. The data was processed in ArcGIS 10.5 in order to create altitudinal profiles and produce hillshade models (shaded relief) of the landscape. We used hillshade models with different illumination and azimuths because some landforms are less visible at certain illumination angles. However, all LiDAR hillshades presented in this article were produced with an illumination of 315° and an azimuth of 45° without any vertical exaggeration.

In this study, we have mapped ancient shorelines and perched deltas and reconstructed the extents, areas and volumes of past ice-dammed lakes. The elevations of the ice-dammed lake shorelines were measured from the LiDAR based terrain models, midway between the inner break and the toe of the shorelines. As the shorelines are tilted, due to differential isostatic uplift following deglaciation, the elevation measurements were used to construct isobases between points of equal elevation of each shoreline. The isobases thus represent contours between sites of equal uplift during a certain length of time (Svendsen and Mangerud, 1987). The shorelines were then projected into a plane perpendicular to the isobases where tilt gradients can be measured directly (Fig. 10).

Approximate areas and volumes of the ice-dammed lakes were calculated in ArcMap 10.5 using the "Surface Volume" tool, which calculates the area and volume of a region between a surface and a reference plane. We used the LiDAR based terrain models as surface and the elevation of the ice-dammed lake shorelines as reference planes. The LiDAR based terrain models were cut according to the mapped extent of the individual ice-dammed lakes. As the shorelines are tilted, we used the mean elevation of the shorelines as reference plane.

4. Results and discussion

4.1. Shorelines from past ice-dammed lakes

Analysis of the LiDAR data reveals the existence of a large number of distinct and long terraces along the valley sides, most of them not previously described in the literature. The terraces can be followed more or less continuously over large areas (30–40 km in length) and in some places correspond with deltaic deposits. We interpret these features to be shorelines formed in large ice-dammed lakes.

In this study, we refer to the entire morphology of the terrace features, from outer slope to inner break, as shorelines regardless of whether they were formed by erosion or deposition. Distinct shoreline segments are typically several hundred meters to several kilometers long with the longest continuous shoreline being 8.7 km long. Shoreline widths commonly range from a few meters to 30 m with the widest one being more than 40 m across. The cross section of most shorelines are inclined by 1–2 m, but the widest (30–40 m) of them can be inclined by as much as 4 m (Fig. 3). The identified shorelines are located on valley sides from 15 to more than 150 m above the present-day valley floors and lakes. As the rivers currently flow toward east or southeast, these high-lying shorelines must have formed in rather deep lakes that were dammed by an ice-barrier in the east. The study area is presented below as three

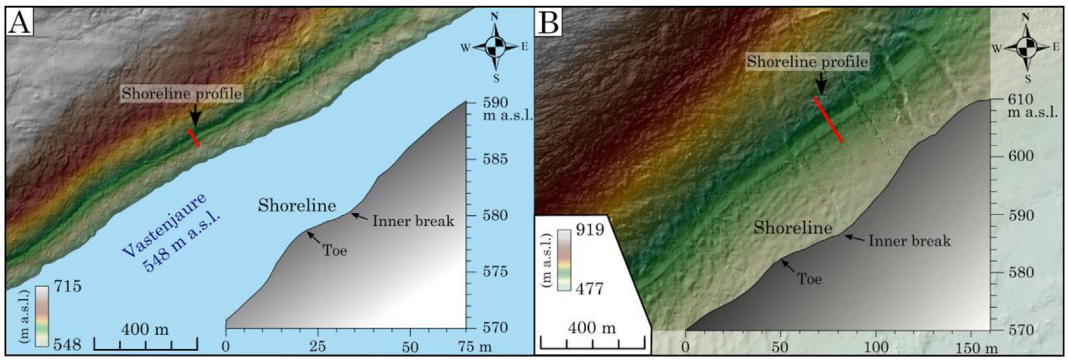

Fig. 3. LiDAR hillshades of two ice-dammed lake shorelines and elevation profiles (red lines). Location is shown in Fig. 4A. A. Shoreline above present-day lake Vastenjaure. The shoreline is *c.* 12 m wide between the toe and inner break and inclined by *c.* 1.5 m. B. Shoreline west of present-day lake Akkajaure. The shoreline is *c.* 30 m wide and inclined by *c.* 4 m. (For interpretation of the references to colour in this figure legend, the reader is referred to the Web version of this article.)

sub-areas containing ice-dammed lake shorelines (Fig. 2).

4.1.1. Shorelines and ice-dammed lakes in Area 1

We have identified traces of several large ice-dammed lakes in Area 1; The three largest lakes were located in the valleys around the present-day Lake Sitasjaure, in the valleys around Lake Akkajaure and around lakes Langas and Satihaure (Fig. 4). These ice-dammed lakes are hereafter referred to as the Sitas Ice Lake, Akka Ice Lake and Langas Ice Lake, respectively (Fig. 4). The highest shoreline (786 m a.s.l.) in Area 1 is located east of Lake Virihaure and the lowest (460 m a.s.l.) at Lake Satihaure.

Around Lake Sitasjaure we have traced a shoreline from an elevation of 673 m a.s.l. in the northwest and up to 692 m a.s.l. in the southeast (Fig. 4A and B). This indicates the shoreline is slightly tilted towards northwest. We did not find shorelines at corresponding elevations in the valley north of the Kallaktjåkko Massif nor around lake Akkajaure. We therefore assume that the Sitas Ice Lake was dammed by ice margins blocking the valley north of the Kallaktjåkkå Massif and in the northwestern end of Lake Akkajaure (Fig. 4A). The surface area of the Sitas Ice Lake is estimated to c. 272 km^2 and the corresponding water volume to c. 14 km^3 (Table 1). LiDAR images were not available around the Sitas Ice Lake's outlet, but it was most likely located in the northern end of the lake, close to the Swedish-Norwegian border. From this pass point, the water must have drained northwestward and into the fjord Skjomen south of the city of Narvik (Fig. 4A).

The largest ice-dammed lake in the study area, the Akka Ice Lake, filled the Akkajaure valley and covered an area of c. 925 km^2 and had a volume of c. 63 km^3 (Table 1). The Akka Ice Lake stretched from the present Lake Akkajaure and southwest into valleys around the present-day lakes Vastenjaure and Virihaure (Fig. 4A and C). The Akka Ice Lake shoreline rises from c. 568 m a.s.l. close to the Swedish-Norwegian border to 591 m a.s.l. at the eastern shore of present-day Lake Akkajaure (Fig. 4A). We could not find a corresponding shoreline further east and we therefore assume that the lake was dammed by an ice margin located close to the eastern end of Akkajaure. The elevation of the shoreline suggests that the outlet of the Akka Ice Lake was located northwest of Lake Akkajaure and that the outlet river drained through the large Hellemobotn canyon (Frödin, 1921) and into Hellemofjorden, leading out to the Norwegian Sea (Fig. 4A).

The Langas Ice Lake is located at lower elevation than the Akka Ice Lake and stretched eastwards from the present-day Lake Akkajaure (Fig. 4A). In the area around Lake Satihaure, there are several shoreline levels that can be traced between 500 and 460 m a.s.l. Along the valley sides around the lakes Langas and Stora Lulevatten there are two distinct shorelines: a higher shoreline at 490–496 m a.s.l. and a lower at 465–473 m a.s.l. (Fig. 4A and D), both dipping slightly towards the northwest. The elevation of the shorelines suggests that the Langas Ice Lake extended into the area of present-day Lake Akkajaure, but it is difficult to identify the shorelines because the lake level was close to the present-day lake level of Akkajaure (Fig. 4A). The Langas Ice Lake shorelines were traced southeastwards to the northern end of Lake Stora Lulevatten and we thus propose that the lake was dammed by an ice tongue that blocked this valley. The elevation of the higher shoreline (490–496 m a.s.l.) suggests that the outlet of the corresponding lake was located east of lake Satihaure (Fig. 4A) whereas the lower shoreline (465–473 m a.s.l.) correspond to a channel in the northern valley side of Stora Lulevatten (Figs. 4A and 5A). The surface area for the highest Langas Ice Lake level is estimated to have been c. 646 km^2 and the lower 576 km^2 (Table 1).

There are also other shorelines suggesting that some smaller ice-dammed lakes existed within Area 1. One shoreline is located at 780 m a.s.l. near the border to Norway west of Lake Akkajaure (Fig. 4A). Another at 786 m a.s.l. suggests that the valley east of Lake Virihaure (southwestern corner of Fig. 4A) was dammed in both ends. A third, somewhat larger lake is inferred from a shoreline at 623 m a.s.l. at Lake Kaitumjaure, in northeastern Area 1. Like the others, this shoreline suggests damming by ice in the east (Fig. 4A).

4.1.2. Shorelines and ice-dammed lakes in Area 2

The shorelines in Area 2 are located around the present-day lakes Sitojaure, Laitaure, Tjaktjajaure and Bievravrre (Fig. 6). Presently these lakes drain towards southeast whilst the higher shorelines indicate a changed drainage pattern due to damming by an ice margin in the valley to the SE. As in Area 1, all shorelines are dipping towards the northwest.

Prominent shorelines occur at four different levels around Lake Sitojaure: 798–800, 753–756, 740–747 and 694–701 m a.s.l. (Fig. 6A and C). Estimated areas and volumes of the ice-dammed lake stages are given in Table 1. The outlet of the first, highest and presumably oldest stage (798–800 m a.s.l.) of this Sitojaure Ice Lake was located northwest of Lake Sitojaure and drained into the northern end of Lake Langas (Fig. 6A). The second lake stage, with shorelines at 753–756 m a.s.l., corresponds to a meltwater channel incised in the valley side just north of the southern end of Lake Sitojaure. Thus, it seems likely that the lake at this time drained northwards to Lake Langas (Figs. 5B and 6A). The third lake stage, at 740–747 m a.s.l., extended some kilometers further to the south. Its outlet river likely drained through a channel a few kilometers east of the outlet of the previous lake stage, but still with a northbound drainage towards Lake Langas (Figs. 5B and 6A). The lowest set of shorelines around Lake Sitojaure (694–701 m a.s.l.) can be traced a

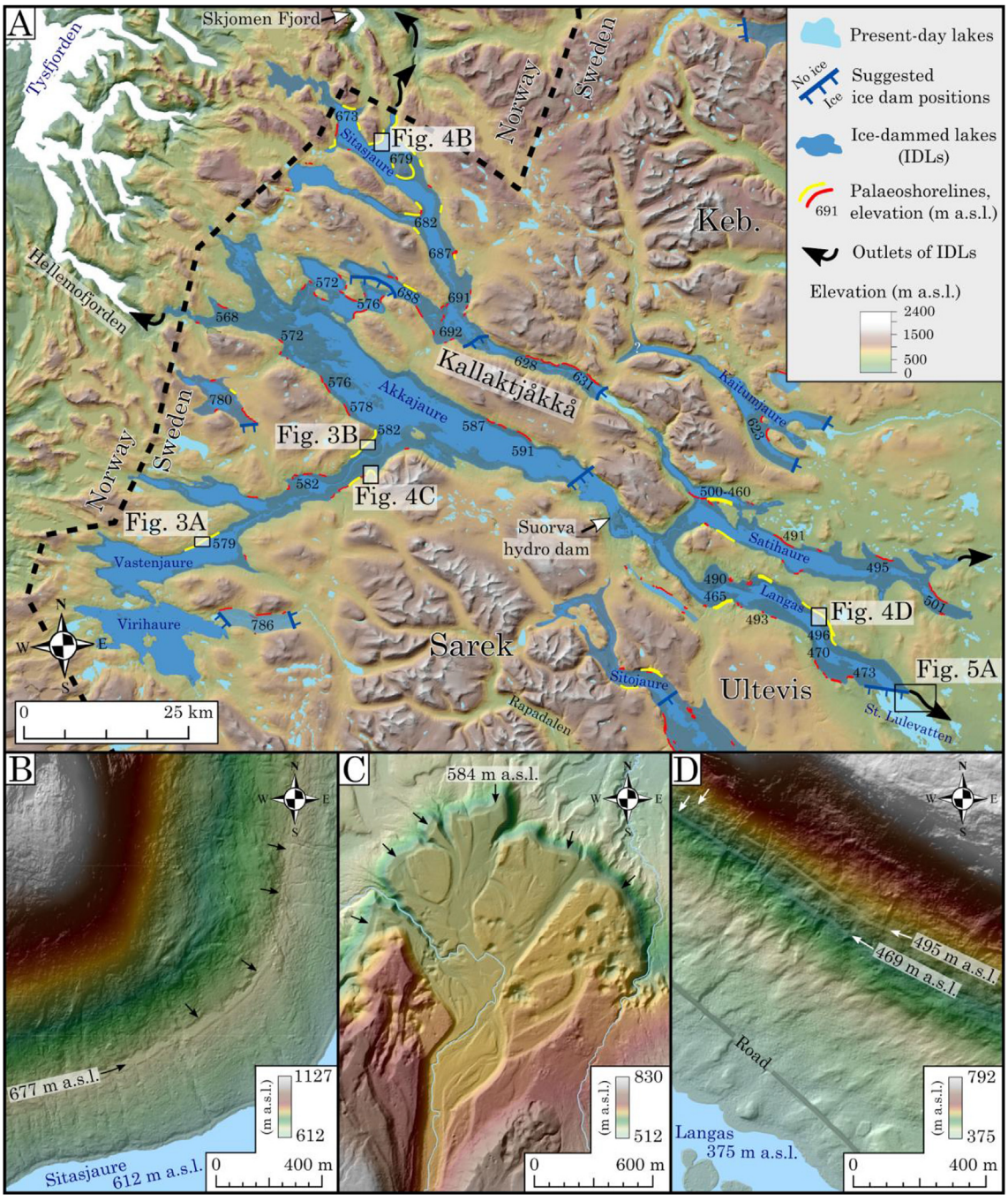

Fig. 4. A. Map of Area 1 (location in Fig. 2) showing the extent of ice-dammed lakes (IDLs) as inferred from mapped shorelines (Background map: EU-DEM v1.1). Previously mapped shorelines (Melander, 1975, 1976, 1982; Hoppe and Melander, 1979) are marked with yellow lines and new shorelines (this study) as red lines. B. LiDAR hillshade of a shoreline (marked with black arrows) above northwestern lake Sitasjaure. The shoreline is locally more than 30 m wide. C. LiDAR hillshade of a perched delta south of lake Akkajaure with a shoreline (marked with black arrows) developed into its front. D. LiDAR hillshade of the two parallel shorelines above lake Langas. (For interpretation of the references to colour in this figure legend, the reader is referred to the Web version of this article.)

little more than 1 km further south. The outlet of the corresponding lake level was probably located southeast of Lake Sitojaure and from there the outlet river drained southwards (Fig. 6A).

Several high-lying shorelines were also found around the lakes Laitaure and Tjaktjajaure. West of lake Laitaure and into the Rapadalen valley, there is a shoreline that can be traced onto former delta surfaces at 558–559 m a.s.l. suggesting ice damming to the east (Fig. 6A). These may also correspond to a shoreline at 563 m a.s.l. above the northwestern shore of present-day Lake Tjaktjajaure, suggesting a larger ice-dammed lake. The outlet must have been located east of Lake Laitaure (Fig. 6A).

Further to the south, there are several lower shoreline generations located around Lake Tjaktjajaure and some well-developed channels in the valley side above the southeastern corner of Lake Tjaktjajaure (Fig. 5C), likely representing additional ice-dammed lakes and their drainage routes. On the southern side of '*Heliga Fallet*' (in English: the Holy Fall) there are shorelines located at an altitude of 438–439 m a.s.l. (Figs. 6A and Fig. 5C) that correspond to

Table 1
Shoreline elevations, volumes and areas as well as the number of elevation measurements along the shorelines and the shoreline gradients along the reference plane (322°N).

Ice-dammed lake	Shoreline elevation (m a.s.l.)	Maximum depth of ice lake[a] (m)	Area (km^2)	Volume (km^3)	Nr. of measuring points	Shoreline gradients (m/km)
Sitas Ice Lake	673–692	113	272	14	61	0.5
Akka Ice Lake	568–591	*c.* 150[b]	925	63	83	0.5
Langas Ice Lake (upper)	490–496	124	646	30	52	0.4
Langas Ice Lake (lower)	465–473	101	576	21	42	0.4
Sitojaure Ice Lake (1st lvl)[c]	800	168	65	5	8	–
Sitojaure Ice Lake (2nd lvl)	753–756	124	62	5	20	0.5
Sitojaure Ice Lake (3rd lvl)	740–747	115	151	12	47	0.4
Sitojaure Ice Lake (4th lvl)	694–701	69	125	6	57	0.4

[a] Depth to present-day lake level.
[b] The present-day lake Akkajaure is regulated by the Sourva hydropower dam (Fig. 3) and its lake level is therefore changing between 423 and 453 m a.s.l.
[c] The shorelines of the 1st level of the Sitojaure Ice Lake are too short to confidently calculate the shoreline gradient.

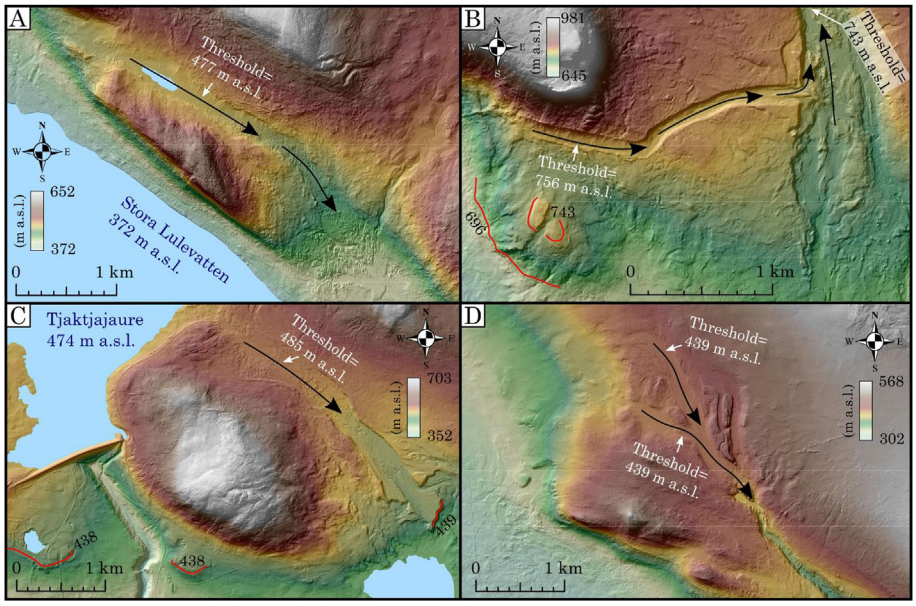

Fig. 5. LiDAR hillshades of different thresholds for outlets of ice-dammed lake outlets. A. Threshold for the outlet of the lower ice-dammed lake level around lake Langas, the Langas Ice Lake (Fig. 4A). B. Thresholds for the outlets of the two middle lake levels of the Sitojaure Ice Lake (Fig. 6A). Red lines mark shorelines and their elevation in meters a.s.l. The higher threshold at 756 m a.s.l. corresponds to shorelines at 753–756 m a.s.l. located further to the west and south (Fig. 6A). The lower threshold at 743 m a.s.l. corresponds to shorelines at 740–747 m a.s.l. C. Threshold for a channel southwest of lake Tjaktjajaure (location in Fig. 6A). No consistent shorelines were found at a corresponding level around Tjaktjajaure but the high elevation of the threshold might suggest an ice-dammed lake to the north. Note the shorelines at 438–439 m a.s.l. to the south, corresponding to a lower ice-dammed lake to the south (Fig. 6A). D. Threshold of the outlet corresponding to the shorelines at 438–439 m a.s.l. south of lake Tjaktjajaure (Fig. 6A). (For interpretation of the references to colour in this figure legend, the reader is referred to the Web version of this article.)

a channel in the valley side to the east (Fig. 5D). Shorelines at this altitude are only found on the northern side of the valley suggesting that the lake was dammed by glacial ice to the south.

In the western end of Lake Bievravvre (lower left corner of Fig. 6A) there is a distinct shoreline at 548 m a.s.l. that truncates several De Geer moraines (Fig. 6B). The De Geer moraines suggests an actively retreating, calving ice front (e.g. De Geer, 1889, 1940; Blake, 2000; Lindén and Möller, 2005; Ottesen and Dowdeswell, 2006). We have not been able to identify clear signs of an outlet from this former ice-dammed lake, but we assume that it spilled over a threshold at this level on the northern side of Lake Bievravvre (Fig. 6A).

4.1.3. Shorelines and ice-dammed lakes in Area 3

Area 3 is the only part of the study area where we have found distinct landforms and deposits that we interpret to stem from a sudden, catastrophic drainage of an ice-dammed lake (described in section 4.2.).

Previous studies have identified high-lying shorelines on the northeastern valley side of Lake Pieskehaure (e.g. Ulfstedt, 1979), in the northern part of Area 3 (Fig. 7A). The northwestern part of Area 3 is currently not covered by LiDAR data, but shorelines at c. 680 m a.s.l can be seen on aerial images northeast of Lake Pieskehaure (Fig. 7B). These features could not be followed around Lake Mavasjaure to the south. However, it is striking that a bedrock threshold at the Swedish/Norwegian border west of Lake Mavasjaure is located at a corresponding elevation (*c.* 680 m a.s.l). We therefore assume that an ice-dammed lake covered both these lakes and that the outlet river was draining into Lake Balvatnet to the west of Lake Mavasjaure (Fig. 7A). As in Area 1 and Area 2, the shoreline indicates that glacier ice was damming the valleys to the southeast of these lakes. Further to the southeast a dense forest cover makes it difficult to identify shorelines, as this region is not yet covered by LiDAR data. However, in a smaller area around the northern end of Lake Tjeggelvas in the eastern part of Area 3, where LiDAR data is available, shorelines occur at 620, 605 and 552 m a.s.l. (Fig. 7A). There is also a perched delta with several shore levels that we interpret to have developed stepwise during a time when the

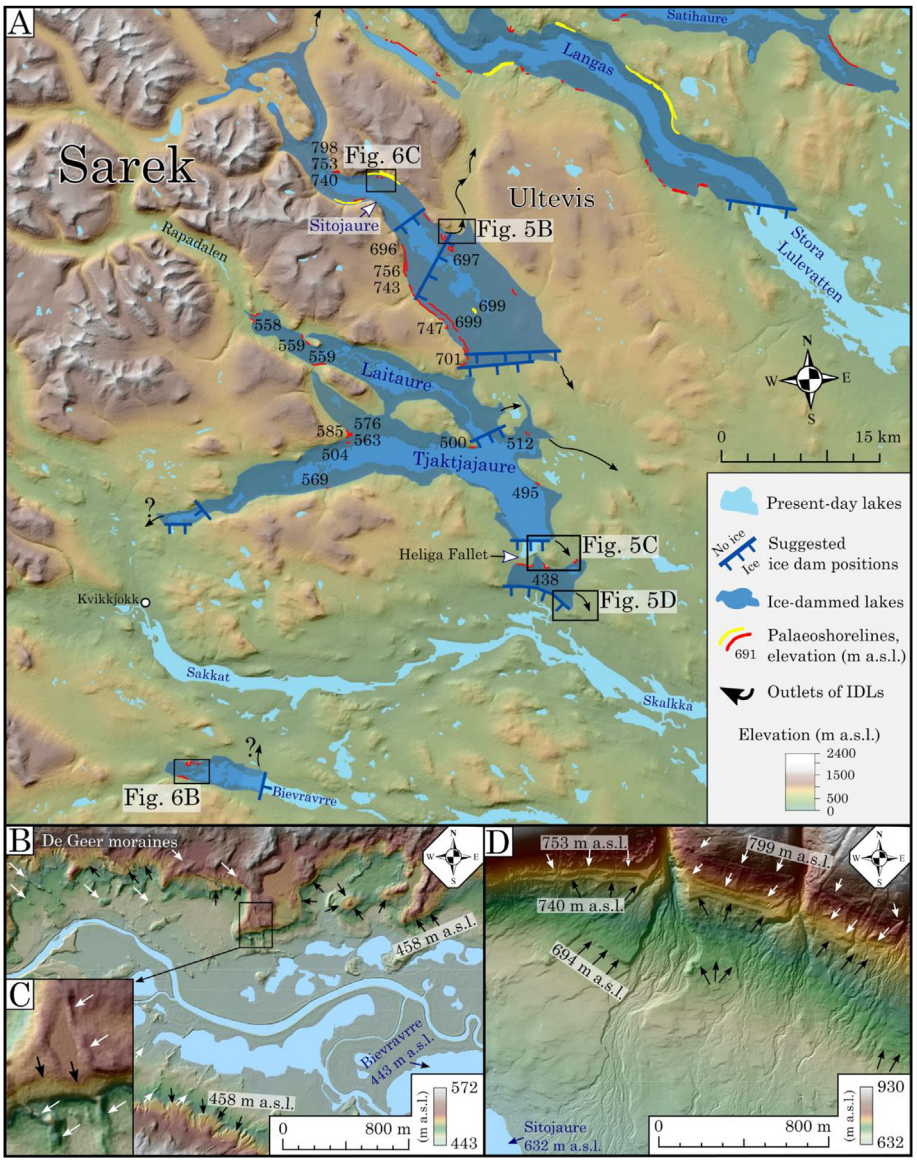

Fig. 6. A. Map of Area 2 (location in Fig. 2) showing the extent of ice-dammed lakes as inferred from mapped shorelines (Background map: EU-DEM v1.1). Previously mapped shorelines (Hoppe and Melander, 1979; Ulfstedt, 1980; Melander, 1982) are marked with yellow lines and new shorelines (this study) as red lines. Around lake Tjaktjajaure are shorelines more scattered and therefore the extent of any ice-dammed lake above Tjaktjajaure uncertain. B. LiDAR hillshades of the western end of lake Bievravrre southeast of Kvikkjokk (Fig. 6A). De Geer moraines are marked with white arrows and a paleoshoreline at 458 m a.s.l. with black arrows. C. Example a shoreline cross-cutting De Geer moraines. D. LiDAR hillshade of four parallel shorelines (black and white arrows) north of lake Sitojaure (Fig. 6A). (For interpretation of the references to colour in this figure legend, the reader is referred to the Web version of this article.)

lake level fell from 644 m a.s.l. down to 573 m a.s.l. (Fig. 7C). These observations from the area around Lake Tjeggelvas therefore suggest high former lake levels, but we are presently unable to reconstruct the corresponding ice-dammed lakes with reasonable certainty.

In the southwestern part of Area 3, in the valleys west-northwest of Lake Hornavan, there are many well-developed high-lying shorelines. Some of the shorelines have been known for over a century and were interpreted to have formed in ice-dammed lakes (Gavelin and Högbom, 1910). We have identified several more shorelines in this area (Fig. 7A). However, these findings only confirm previous reconstructions with minor changes and we have therefore chosen not to do more with these lakes, except for demonstrating their former existence.

4.2. Glacial lake outburst flood deposits along Pite River valley

In the southeastern end of Lake Tjeggelvas, where the Pite River starts, lies the large Abbmo boulder deposit (Figs. 7A and 8B). Downstream of Abbmo, additional large boulder deposits can be seen along the Pite River Valley as well as areas of stream-washed bedrock high above the present-day river level. Some of these deposits have previously been studied and explained to be the result of several drainages of ice-dammed lakes during the deglaciation (Elfström, 1983, 1987; 1988). The LiDAR data have now made possible more detailed mapping of features characteristic of large-scale floods in this densely forested area.

Using LiDAR data, we have traced large erosional and depositional landforms continuously for some 130 km along the Pite River valley from Abbmo in the northwest to Gransel, west of Vidsel in

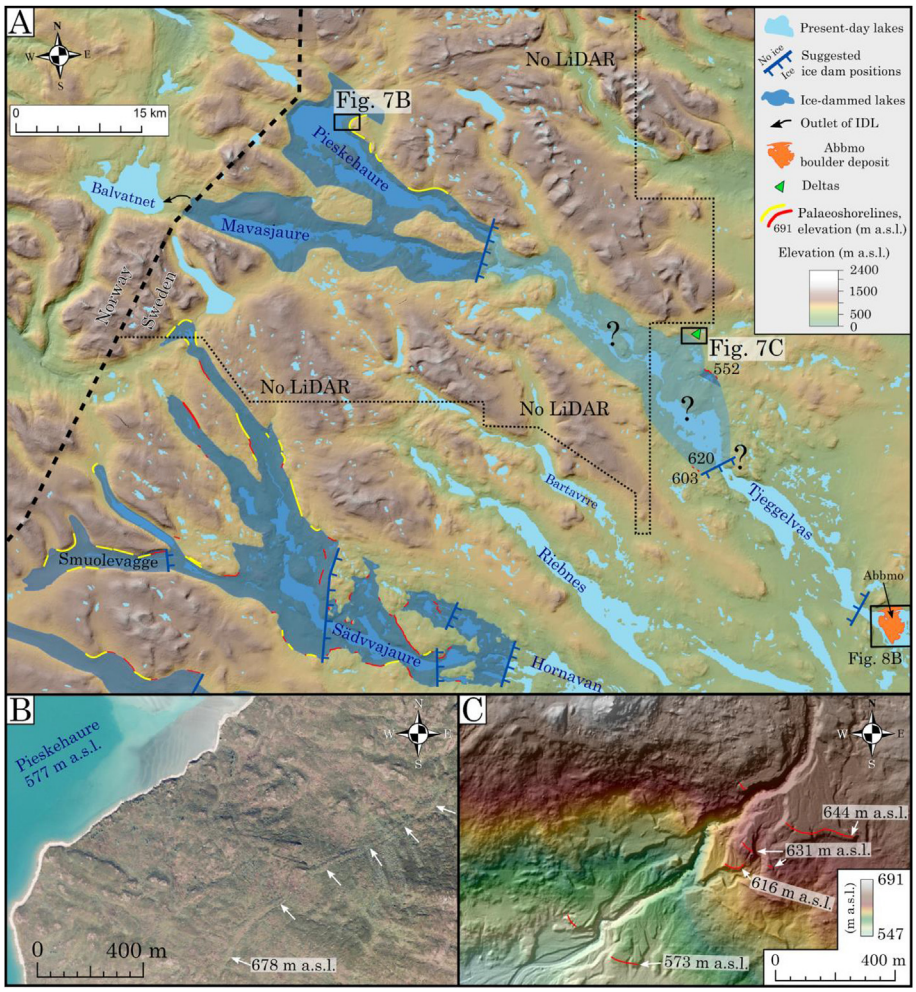

Fig. 7. A. Map of Area 3 (location in Fig. 2) showing the extent of ice-dammed lakes as inferred from mapped shorelines (Background map: EU-DEM v1.1). Previously mapped shorelines (Gavelin and Högbom, 1910; Ulfstedt, 1977, 1979) are marked with yellow lines and new shorelines (this study) as red lines. The northwestern part of Area 3 is currently not covered by LiDAR data, hampering identification of potential shorelines located there. B. Aerial image of a shoreline (marked by white arrows) above lake Pieskehaure. C. LiDAR hillshade of delta deposits northwest of lake Tjeggelvas. (For interpretation of the references to colour in this figure legend, the reader is referred to the Web version of this article.)

the southeast (Figs. 8 and 9). Large streamlined deposits, interpreted as longitudinal flood bars, are found along the valley floor (Fig. 8). Some of these are several kilometers long and the most morphologically distinct ones we have classified as pendant bars. The pendant bars are found on the leeside of flood flow projections, such as bedrock protrusions, or around valley bends where stream capacity decreased and favored deposition (Fig. 8). The bedrock is often exposed on the outside of valley bends an on bedrock protrusions, as superficial deposits were washed away during the GLOF. The uppermost flooded level is indicated by a clear removal of superficial deposits on the valley sides which can be seen up to 50 m above the present-day river level (Fig. 9). We have traced these prominent flood-related landforms continuously along the Pite River Valley and therefore disagree with the interpretation by Elfström (1988), who suggested that the landforms formed during several consecutive floods. Instead, we interpret the landforms to stem from one single event of a catastrophic GLOF. As the westernmost GLOF-landforms are found at Abbmo, the ice-dammed lake must have been located in the mountain valleys northwest of Abbmo (Fig. 7). The catastrophic outflow of water seems to have flowed unobstructed down the Pite River Valley and emptied into the large early Holocene Ancylus Lake that occupied the Baltic Sea Basin at the time (Björck, 1995).

4.3. Postglacial shoreline gradients and uplift pattern

In northern Scandinavia, observations of the early Holocene postglacial uplift pattern are currently only available from shoreline data along the Norwegian and the Baltic Sea coasts (e.g. Eronen and Ristaniemi, 1992; Møller, 1987, 2003; Lindén et al., 2006). Therefore, the gradients of the ice-dammed lake shorelines provide critical information about the glacio-isostatic rebound from the inland area where no such observations currently exist.

The many distinct shorelines belonging to the Akka Ice Lake in Area 1 (Fig. 4A) made it possible to reconstruct uplift isobases, tilt direction and shoreline gradients (Table 1, Fig. 10). The shorelines are tilted towards northwest, consistent with the early Holocene uplift pattern for the adjacent coast of Norway (Møller, 1987, 2003). When the shoreline elevations from the three largest ice-dammed lakes in Area 1 were projected into the projection plane (322°N) and shoreline diagrams constructed (Fig. 10), the shoreline gradients were found to be ranging from 0.5 m/km for the oldest to 0.4 m/km for youngest (Fig. 10C). The shorelines of the Sitojaure Ice Lake, in Area 2, were also projected into a projection plane with the same direction (322°N) and they display similar gradients ranging from 0.5 to 0.4 m/km (Fig. 10D).

We have compiled the Lateglacial and Holocene shoreline

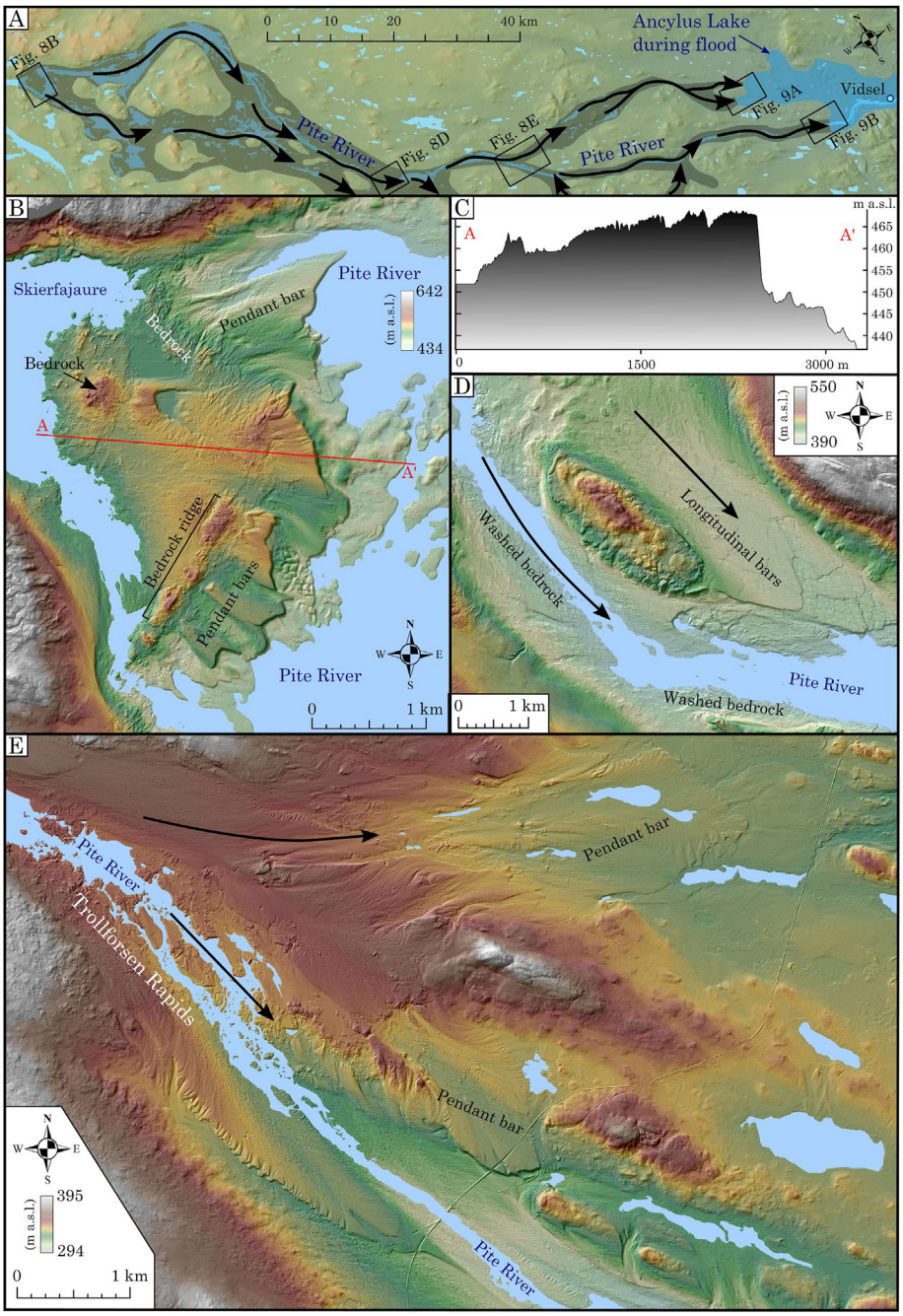

Fig. 8. A. Map showing the extent (grey) and the drainage routes (black arrows) of the GLOF along Pite River (Background map: EU-DEM v1.1). B. LiDAR hillshade of the Abbmo boulder deposit. Note the washed bedrock (rugged areas) and large pendant bars (smooth areas). C. Elevation profile across the Abbmo boulder deposit (Fig. 8B). Note that the distal slope of the pendent bar is c. 20 m high. D. LiDAR hillshade of longitudinal bars and washed bedrock. The GLOF-routes is marked by black arrows. E. LiDAR hillshade of the Trollforsen Rapids where the GLOF flooded into a neighbouring valley to the north.

displacement data (Eronen and Ristaniemi, 1992; Møller, 1987, 2003; Lindén et al., 2006) and reconstructed the pattern of glacio-isostatic uplift along a c. 1400 km long northwest-southeast transect from the Norwegian Sea to Lake Ladoga (Fig. 11). This reconstruction shows that our area is located well west of the uplift center. Below we will use this diagram to estimate the age of the ice-dammed lakes (Section 4.4).

4.4. Age and duration of the ice-dammed lakes

Presently, the most direct method to date the lakes is the cross-cutting relation between the GLOF-landforms and shorelines of the Ancylus Lake in the Baltic Sea basin (Figs. 8 and 9). West of the village Vidsel, erosive lines from the drainage cross-cut Ancylus Lake shorelines at an elevation of c. 165 m a.s.l. whereas below 155 m a.s.l. Ancylus-shorelines are developed in the GLOF deposits (Fig. 9). Thus, we conclude that the drainage took place after the formation of the 165 m shoreline but before formation of the 155 m Ancylus-Lake shorelines (Figs. 9 and 12A).

Lindén et al. (2006) constructed a relative sea-level curve for a site located c. 25 km southeast of our site, i.e. closer to the center of isostatic uplift. Using this curve and adjusting our shoreline

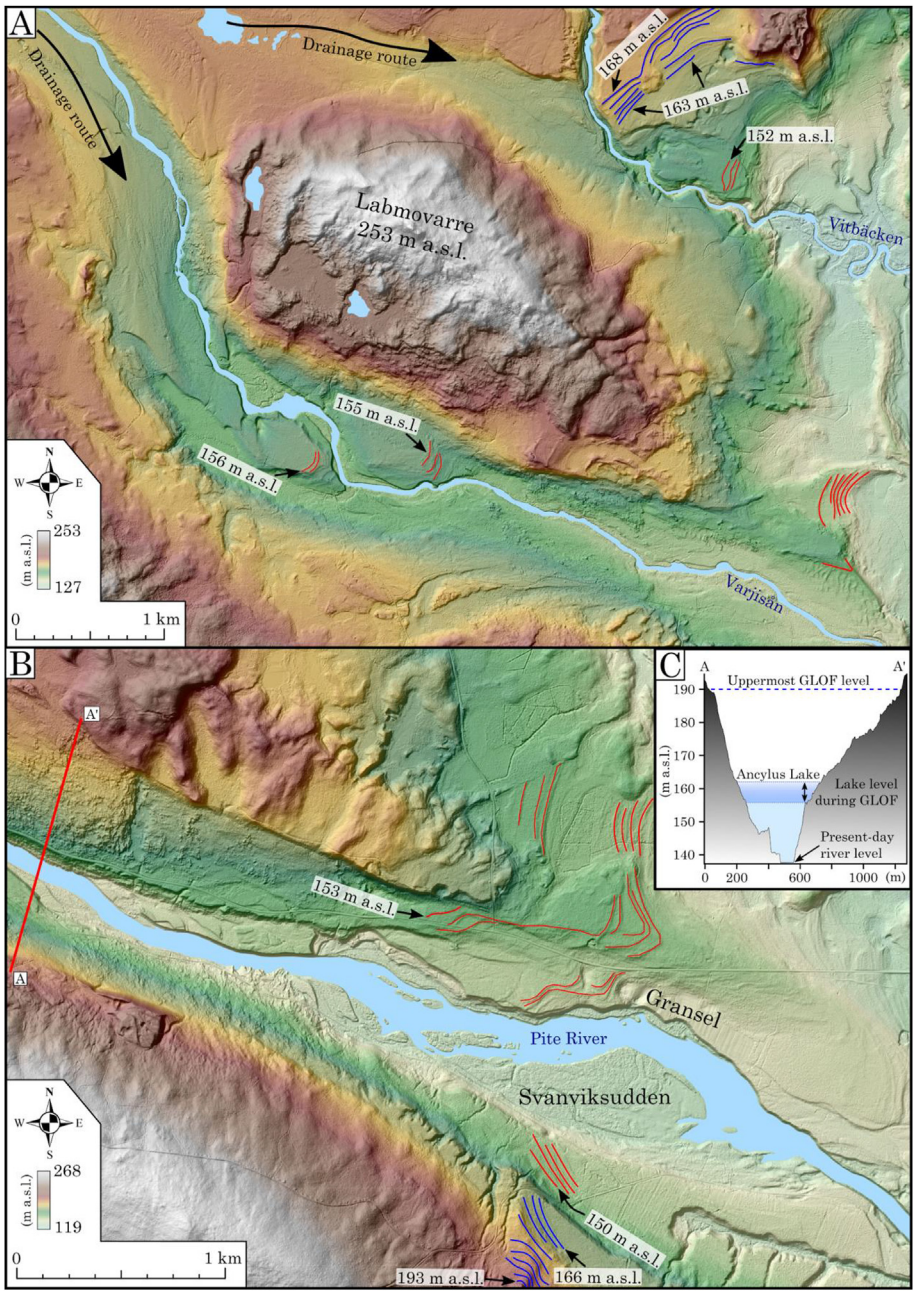

Fig. 9. LiDAR hillshades of two area west of Vidsel, where the GLOF ended into the early Holocene Ancylus Lake (Fig. 8A). A and B. Note that the higher shorelines (blue lines) are cut by the flood, whereas the lower shorelines are developed in GLOF deposits (red lines). C. Elevation profile across the Pite River. The uppermost flood level, as inferred from erosive lines, are located up to 50 m above present day river level. Considering the elevation of paleoshorelines above and below the flood, the Ancylus Lake level was located between *c.* 165-155 m a.s.l. during the flood. The water level in the valley thus rose by *c.* 30 m during the flood. (For interpretation of the references to colour in this figure legend, the reader is referred to the Web version of this article.)

altitudes for tilting according to the tilting model of Lindén et al. (2006), the age of the GLOF can be estimated to 10.3–9.9 ka cal. BP (Fig. 11). This age should represent the very end of ice-dammed lakes in Area 3.

Another method for estimating the age of the ice-dammed lakes in Area 1 and Area 2 is to compare their shoreline gradients with the gradients of dated marine shorelines in adjacent northern Norway (Fig. 11). The ice-dammed lake shorelines are of course located at much higher elevation than the marine shorelines, but the tilt of contemporaneous shorelines have to be the same within a given region as the differential uplift has affected both marine and lacustrine shorelines equally. As seen from Fig. 11, the oldest and westernmost ice-dammed lake shorelines partly overlap with the marine shorelines. However, the ice-dammed lake shoreline is less tilted (0.5 m/km) than the 10.2 cal ka BP Norwegian-coast shoreline, *c.* 0.7 m/km (Møller, 2003), indicating that these ice-dammed lakes formed after 10.2 cal ka BP.

The decreasing tilt of the ice-dammed lake shorelines from *c.* 0.5 m/km for the oldest to 0.4 m/km for the youngest (Fig. 10) should provide temporal information of the ice-dammed lakes' existence. The early Holocene marine shorelines along the adjacent coast of Norway are not precisely mapped or dated, but their tilt

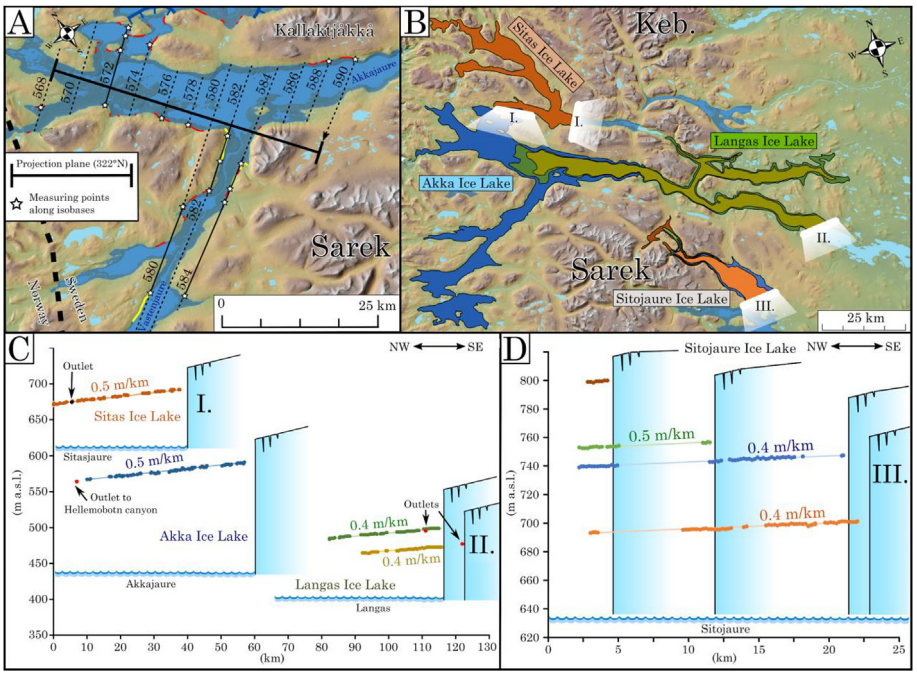

Fig. 10. A. Isobases with elevations (m a.s.l.) for the Akka Ice Lake (Background map: EU-DEM v1.1). Solid black lines mark isobases drawn between several measuring points of same elevation. Dashed black lines either mark extrapolated isobases from single measuring points or interpolated isobases between measuring points. The projection plane has an azimuth of 322°N. B. Extents of the ice-dammed lakes. Schematic ice margins (white) mark where the lakes are believed to have been dammed and are numbered (I-III) in chronological order. C and D. Shoreline gradients and schematic ice margins (not to scale).

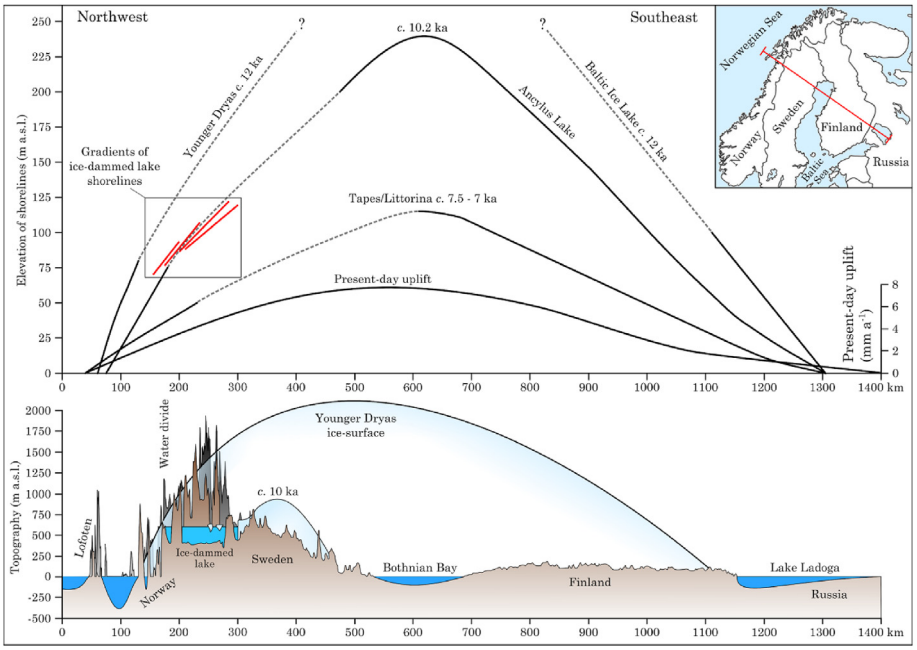

Fig. 11. Upper panel show Lateglacial and Holocene shoreline elevations along a transect from the Norwegian Sea to Lake Ladoga in northwest Russia (Eronen and Ristaniemi, 1992; Møller, 1987, 2003; Lindén et al., 2006) as well as the present-day uplift (Ågren and Svensson, 2007). Dashed lines are interpolated over areas where no previous observations currently exist. All ages are given in cal. ka BP. The gradients of the ice-dammed lake shorelines (this study) are shown as red lines. Lower panel show the topography across the transect, the Younger Dryas ice-profile (Patton et al., 2017) and a tentative c. 10 cal. ka BP ice-surface with ice-dammed lakes. (For interpretation of the references to colour in this figure legend, the reader is referred to the Web version of this article.)

apparently changed with a rate of 0.020–0.025 m/km per 100 years around 10.2–10.0 cal ka BP (Fig. 13) (Møller, 2003). The difference between the oldest and youngest ice-dammed lake shoreline is *c.* 0.2 m/km, and assuming that the tilt of the ice-dammed lake shorelines changes with a similar rate as the marine shorelines, this suggests a time span of several centuries between the oldest and the youngest ice-dammed lake in Area 1. The broad and well developed shorelines support a formation time of some length.

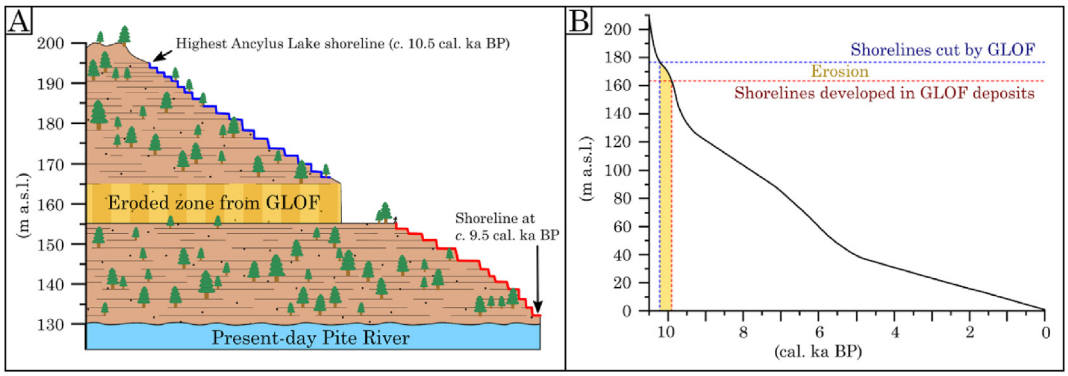

Fig. 12. A. Schematic profile of the area where early Holocene shorelines were truncated by the GLOF. B. Relative sea-level curve (black line) for coastal Norrbotten, modified from Lindén et al. (2006). Elevation of the lowest shorelines cut by the flood (blue) and the highest shorelines developed in the flood deposits (red) are plotted as horizontal dashed lines. The elevation of the shorelines are corrected for differential uplift between the site of Lindén et al. (2006) and our site. The age of the flood is read from where the horizontal lines (blue and red) cross the relative sea-level curve (black). Accordingly, the age of the flood is constrained to 10.3–9.9 cal ka BP. (For interpretation of the references to colour in this figure legend, the reader is referred to the Web version of this article.)

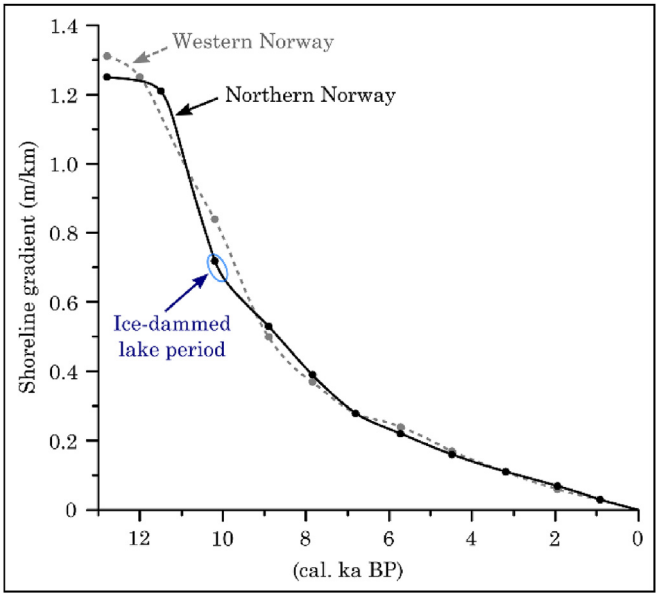

Fig. 13. Shoreline gradients plotted against age for western (Svendsen and Mangerud, 1987) respectively northern Norway (based on Møller, 1987, 2003). The curve for northern Norway corresponds to the transect shown in Fig. 11. The ice-dammed lakes are inferred to have been active after 10.2 cal ka BP when the shoreline gradients in northern Norway changed with c. 0.020–0.025 m/km per 100 years.

4.5. Pattern and age of final deglaciation of the Scandinavian Ice Sheet

Our data reveal a pattern of large ice-dammed lakes in northern Sweden that can only be explained by an eastward retreating ice sheet margin with ice-dammed lakes formed in deglaciated valleys between the water divide and the ice margin (Figs. 4, Fig. 6, Fig. 7). The distribution of the ice-dammed lakes suggest that the ice sheet retreated away from the Sarek and Sulitelma Mountains towards the southeast (Fig. 14), which is in contrast with the assumption that the last ice sheet remnants retreated into the mountains of eastern Sarek, as recently suggested by e.g. Stroeven et al. (2016). We consider the westernmost GLOF landforms, at Abbmo (Fig. 8B), and the westernmost extent of the large coherent eskers in the lowland east of the mountain range to reflect the eastern ice margin during the final phase of deglaciation (Fig. 14).

Previous works, which argued for final deglaciation in the higher mountain massifs (e.g. Hoppe, 1959; Lundqvist, 1972; 1986; Kleman, 1990, 1992; Stroeven et al., 2016), were mainly based on interpretation of glacial striae and streamlined landforms. However, as large parts of the ice sheet was cold-based during the last deglaciation of northern Sweden, the glacial erosion would have been minimal. The streamlined features could thus be preserved landforms from earlier phases in the Weichselian glaciation, when the ice-divide was located further west. (e.g. Lagerbäck, 1988; Rodhe, 1988; Kleman, 1992; Kleman and Stroeven, 1997; Hättestrand, 1998; Kleman and Hättestrand, 1999; Fabel et al., 2002, 2006; Fredin and Hättestrand, 2002). For example, as Lagerbäck (1988) pointed out, there are in some areas minute glacial striae on polished bedrock outcrops formed earlier in the Weichselian glaciation preserved whilst striae from the last deglaciation are lacking. The use of striations and streamlined landforms for interpreting deglacial patterns should therefore be used with extra caution in this area.

If there was minimal glacial erosion during the final deglaciation, the question arises whether or not the ice-dammed lake shorelines also are older, preserved features. We find this possibility very unlikely for several reasons. A weighty argument against this is the fact that the shorelines are traceable more or less continuously over large areas and have a fresh appearance with sharp boundaries against the till surfaces into which they are incised. Further, the shorelines are also consistent with the early Holocene marine shorelines along the northern Norwegian coast in the west (section 4.3.). But the most important argument for the ice-dammed lakes being formed during the last deglaciation are the undisputable traces left by the associated GLOF along the Pite River Valley (Figs. 8 and 9). As these occur within a sequence of the early Holocene Ancylus lake shorelines (section 4.4.) it can be ruled out that they are preserved from earlier in the Weichselian glaciation.

Furthermore, from a climatic point of view we consider a deglaciation into smaller active ice caps in the higher mountain massifs as unlikely during the early Holocene. We note that the summer insolation during 10–9 cal ka BP was at its Holocene maximum (Berger, 1978; Berger and Loutre, 1991) and birch forests established across the entire northern Scandinavia (Sjögren and Damm, 2018). We therefore find it more likely that the entire ice sheet was out of phase with the prevailing climate with an equilibrium line altitude located above the entire ice sheet. The warm climate hence hampered ice build-up in the mountains and, instead, the ice sheet retreated eastward across the water divide

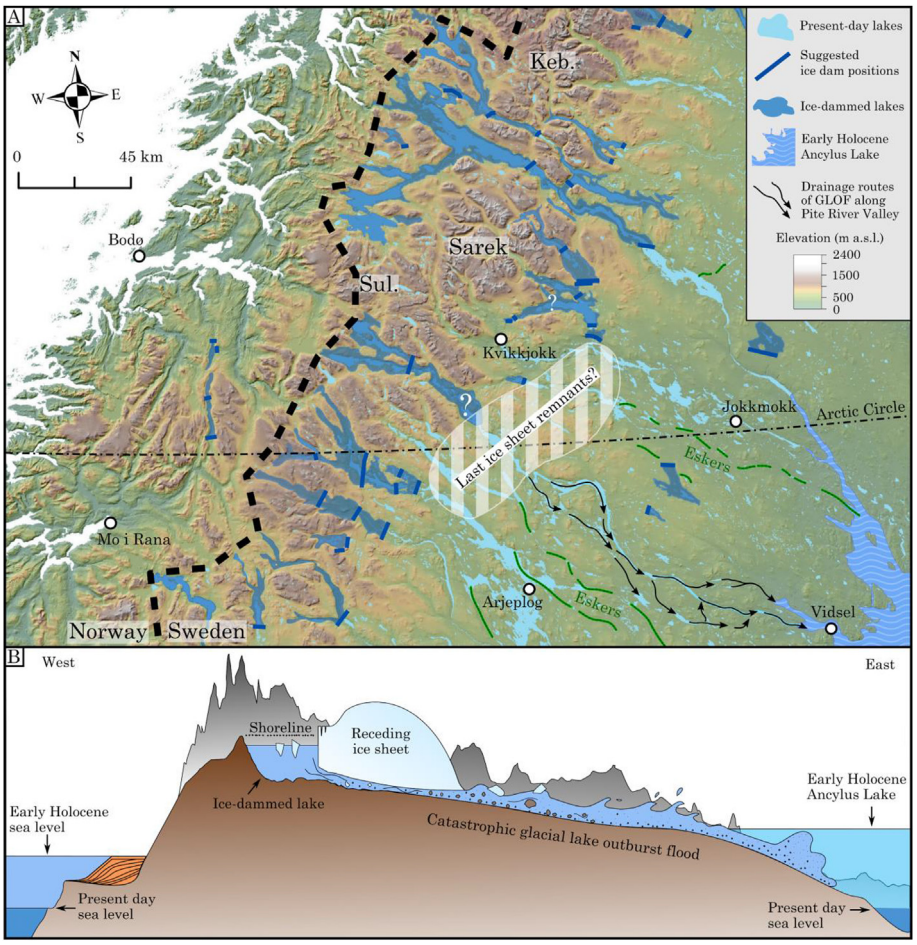

Fig. 14. A. Map showing the suggested location of the last Scandinavian Ice Sheet remnants south east of the Sarek mountains (Background map: EU-DEM v1.1). B. Schematic profile of the early Holocene catastrophic glacial lake outburst flood (GLOF) along the Pite River Valley.

with the higher mountains probably melting out as nunataks. As the ice sheet retreated across the water divide, ice-dammed lakes formed in front of the ice margin. We suggest that these lakes additionally may have triggered positive feedback mechanisms promoting ice loss. The ice-dammed lakes would have lowered the effective pressure at the ice-bed interface, and thereby resulted in glacier speed-up and thinning of the ice sheet. The tinning would then cause the ice margins to float, leading to calving and, in turn, increased loss of ice (e.g. Kirkbride, 1993; Boyce et al., 2007; Tsutaki et al., 2011, 2013).

Based on our results, we cannot say whether the ice sheet disintegrated into several individual ice caps or if it remained as a coherent ice mass. Nor can we completely ignore the possibility that smaller ice masses remained within the higher mountains. However, in our view the ice-dammed lakes demonstrate that the ice margin retreated towards the previous ice divide of ice sheet that was located east of the water shed, and that there was no westward migration of the ice divide or any buildup of larger ice caps in the mountain range. Accordingly, we conclude that the last coherent ice sheet remnants melted away east of the mountain range shortly after 10.3–9.9 cal ka BP (Fig. 14).

5. Conclusions

- We document a number of shorelines from early Holocene ice-dammed lakes in northern Sweden.
- The lakes were dammed between the main water divide to the west and the retreating ice margin to the east.
- The distribution of the ice-dammed lakes shows that the last remnant of the Scandinavian Ice Sheet was located east of the mountain range and not in the higher mountains.
- Large deposits and erosional landforms from a large glacial lake outburst flood (GLOF) are mapped along the Pite River Valley.
- The GLOF is dated to 10.3–9.9 cal ka BP, based on cross-cutting relations between flood landforms and raised shorelines in the Baltic Sea basin.
- We consider this age interval to be representative also for the last ice sheet remnants in northern Sweden.

Acknowledgments

This work was financially supported by The Research Council of Norway and is a contribution to the project “Climate History along the Arctic Seaboard of Eurasia (CHASE)” (NRC 255415). This study is also a contribution to the RISES project on Quantifying and understanding rates of ice sheet change and the Bjerknes Centre for Climate Research in Bergen, Norway. We acknowledge Mark Johnson for improving the English language and Helena Alexanderson and an anonymous reviewer for their constructive reviews that helped improve the manuscript.

Appendix A. Supplementary data

Supplementary data to this article can be found online at https://doi.org/10.1016/j.quascirev.2019.105862.

References

Ågren, J., Svensson, R., 2007. Postglacial land uplift model and system definition for the new Swedish height system RH 2000. Lantmäteriet-Rapp. 2007, 4.

Berger, A.L., 1978. Long-term variations of caloric insolation resulting from the earth's orbital elements. Quat. Res. 9, 139–167. https://doi.org/10.1016/0033-5894(78)90064-9.

Berger, A., Loutre, M.F., 1991. Insolation values for the climate of the last 10 million years. Quat. Sci. Rev. 10, 297–317. https://doi.org/10.1016/0277-3791(91)90033-Q.

Björck, S., 1995. A review of the history of the Baltic Sea, 13.0-8.0 ka BP. Quat. Int. 27, 19–40. https://doi.org/10.1016/1040-6182(94)00057-C.

Blake, K.P., 2000. Common origin for De Geer moraines of variable composition in Raudvassdalen, northern Norway. J. Quat. Sci. 15, 633–644. https://doi.org/10.1002/1099-1417(200009)15:6<633::AID-JQS543>3.0.CO;2-F.

Boulton, G., Dongelmans, P., Punkari, M., Broadgate, M., 2001. Palaeoglaciology of an ice sheet through a glacial cycle: the European ice sheet through the Weichselian. Quat. Sci. Rev. 20, 591–625. https://doi.org/10.1016/S0277-3791(00)00160-8.

Boyce, E.S., Motyka, R.J., Truffer, M., 2007. Flotation and retreat of a lake-calving terminus, Mendenhall Glacier, southeast Alaska, USA. J. Glaciol. 53, 211–224. https://doi.org/10.3189/172756507782202928.

De Geer, G., 1889. Mötet den 5 December 1889. Geol. Fören. Stock. Förhandlingar 11, 395–400. https://doi.org/10.1080/11035898409443539.

De Geer, G., 1940. Geochronologia suecica principles. K. Sven. Vetensk. Handl. III 18 (6), 1–367.

Elfström, Å., 1983. The Båldakatj boulder delta, Lapland, northern Sweden. Geogr. Ann. Ser. A, Phys. Geogr. 65, 201–225. https://doi.org/10.1080/04353676.1983.11880087.

Elfström, Å., 1987. Large boulder deposits and catastrophic floods. Geogr. Ann. Ser. A Phys. Geogr. 69, 101–121. https://doi.org/10.1080/04353676.1987.11880200.

Elfström, Å., 1988. Late glacial hydrology of the upper Pite River valley, Swedish Lapland. Geogr. Ann. Ser. A Phys. Geogr. 70, 99–123. https://doi.org/10.1080/04353676.1988.11880242.

Eronen, M., Ristaniemi, O., 1992. Late quaternary crustal deformation and coastal changes in Finland. Quat. Int. 15–16, 175–184. https://doi.org/10.1016/1040-6182(92)90045-4.

Fabel, D., Stroeven, A.P., Harbor, J., Kleman, J., Elmore, D., Fink, D., 2002. Landscape preservation under Fennoscandian ice sheets determined from in situ produced 10Be and 26Al. Earth Planet. Sci. Lett. 201 (2), 397–406. https://doi.org/10.1016/S0012-821X(02)00714-8.

Fabel, D., Fink, D., Fredin, O., Harbor, J., Land, M., Stroeven, A.P., 2006. Exposure ages from relict lateral moraines overridden by the Fennoscandian ice sheet. Quat. Res. 65, 136–146. https://doi.org/10.1016/j.yqres.2005.06.006.

Fredin, O., Hättestrand, C., 2002. Relict lateral moraines in northern Sweden—evidence for an early mountain centred ice sheet. Sediment. Geol. 149, 145–156. https://doi.org/10.1016/S0037-0738(01)00249-4.

Frödin, J., 1921. De senglaciala isdämda sjöarna i örorsta delen av Stora Lule älvs flodområde och deras dräneringsvägar. Geol. Fören. Stock. Förh. 43, 53–69. https://doi.org/10.1080/11035892109443888.

Gavelin, A., Högbom, A.G., 1910. Norra Sveriges Issjöar. En Sammanställning Af Hittills Gjorda Undersökningar, vol. 7. Sveriges Geologiska Undersökning, Ca.

Hansen, A.M., 1886. Om seter eller strandlinjer i store høider over havet. Archiv Math. Nat. 10, 329–352.

Holmsen, G., 1915. Brædæmte sjøer i Nordre Østerdalen. Nor. Geol. Unders. 73, 211.

Hoppe, G., 1959. Glacial morphology and inland ice recession in northern Sweden. Geogr. Ann. 41, 193–212. https://doi.org/10.1080/20014422.1959.11907951.

Hoppe, G., Melander, O., 1979. Geomorphological map 28 I Stora Sjöfallet - description and assessment of areas of geomorphological importance. Statens Naturvårdsv. PM 1207, 48.

Hughes, A.L.C., Gyllencreutz, R., Lohne, Ø.S., Mangerud, J., Svendsen, J.I., 2016. The last Eurasian ice sheets - a chronological database and time-slice reconstruction, DATED-1. Boreas 45, 1–45. https://doi.org/10.1111/bor.12142.

Hättestrand, C., 1998. The Glacial Geomorphology of Central and Northern Sweden. Sveriges Geologiska Undersökning, pp. 1–47. Ca 85.

Høgaas, F., Longva, O., 2016. Mega deposits and erosive features related to the glacial lake Nedre Glomsjø outburst flood, southeastern Norway. Quat. Sci. Rev. 151, 273–291. https://doi.org/10.1016/j.quascirev.2016.09.015.

Høgaas, F., Longva, O., 2018. The late-glacial ice-dammed lake Nedre Glomsjø in Mid-Norway: an open lake system succeeding an actively retreating ice sheet. Nor. J. Geol. 98, 1–15. https://doi.org/10.17850/njg98-4-08.

Högbom, A.G., 1892. Om märken efter isdämda sjöar i Jemtlands fjelltrakter. Geol. Fören. Stock. Förh. 14, 561–582. https://doi.org/10.1080/11035899209445449.

Karlén, W., 1979. Deglaciation dates from northern Swedish Lappland. Geogr. Ann. Ser. A Phys. Geogr. 61, 203–210. https://doi.org/10.1080/04353676.1979.11879991.

Karlén, W., 1981. ^{14}C datering av Norrbottens deglaciation. IGCP project 7311/24. In: Symposium 12-13 January 1981. Den senaste Nedisningens Förlopp Med Särskild Hänsyn till Deglaciationen I Sverige. Stockholm, pp. 96–100.

Kirkbride, M.P., 1993. The temporal significance of transitions from melting to calving termini at glaciers in the central Southern Alps of New Zealand. Holocene 3 (3), 232–240. https://doi.org/10.1177/095968369300300305.

Kleman, J., 1990. On the use of glacial striae for reconstruction of paleo-ice sheet flow patterns- with application to the Scandinavian ice sheet. Geogr. Ann. 72 (3–4), 217–236. https://doi.org/10.1080/04353676.1990.11880318.

Kleman, J., 1992. The palimpsest glacial landscape in northwestern Sweden: late Weichselian deglaciation landforms and traces of older west-centered ice sheets. Geogr. Ann. Ser. A Phys. Geogr. 74 (4), 305–325. https://doi.org/10.2307/521429.

Kleman, J., Hättestrand, C., 1999. Frozen-bed Fennoscandian and Laurentide ice sheets during the last glacial maximum. Nature 402 (6757), 63. https://doi.org/10.1038/47005.

Kleman, J., Hättestrand, C., Borgström, I., Stroeven, A., 1997. Fennoscandian palaeoglaciology reconstructed using a glacial geological inversion model. J. Glaciol. 43 (144), 283–299. https://doi.org/10.3189/S0022143000003233.

Kleman, J., Stroeven, A.P., 1997. Preglacial surface remnants and Quaternary glacial regimes in northwestern Sweden. Geomorphology 19 (1–2), 35–54. https://doi.org/10.1016/S0169-555X(96)00046-3.

Lagerbäck, R., 1988. The Veiki moraines in northern Sweden-widespread evidence of an Early Weichselian deglaciation. Boreas 17 (4), 469–486. https://doi.org/10.1111/j.1502-3885.1988.tb00562.x.

Lantmäteriet, 2019. Product Description: GSD-Elevation Data, Grid 2+, Document Version: 2.5. https://www.lantmateriet.se/globalassets/kartor-och-geografisk-information/hojddata/e_grid2_plus.pdf.

Lindén, M., Möller, P., 2005. Marginal formation of De Geer moraines and their implications to the dynamics of grounding-line recession. J. Quat. Sci. 20, 113–133. https://doi.org/10.1002/jqs.902.

Lindén, M., Möller, P., Björck, S., Sandgren, P., 2006. Holocene shore displacement and deglaciation chronology in Norrbotten, Sweden. Boreas 35 (1), 1–22. https://doi.org/10.1111/j.1502-3885.2006.tb01109.x.

Linnæus, C., Caroli Linnaei, P.S.R., 1734. Iter Dalekarlicum jussu et impensis Viri Generosissimi et Excellentissimi Dni Nicolai Reuterholmi Gubernatoris Provincie Dalekarlicae institutum per Dalekarlicam Sveciae provinciam quoad orientalem, pp. 1–224. Alp. Occident. partem, observationibus constans Geogr. Phys. Mineral. Bot. Zool. Domest. Oecon. quotidie collect. mensi Julii die 3 ad Augusti d. 17 Anni 1734.

Longva, O., 1994. Flood Deposits and Erosional Features from the Catastrophic Drainage of Preboreal Glacial Lake Nedre Glåmsjø. Department of Geology, University of Bergen, SE Norway (PhD thesis).

Lundqvist, J., 1972. Ice-lake types and deglaciation pattern along the Scandinavian mountain range. Boreas 1 (1), 27–54. https://doi.org/10.1111/j.1502-3885.1972.tb00142.x.

Lundqvist, J., 1986. Late Weichselian glaciation and deglaciation in Scandinavia. Quat. Sci. Rev. 5, 269–292. https://doi.org/10.1016/0277-3791(86)90192-7.

Melander, O., 1975. Geomorphological map 28G Virihaure- Description and assessment of areas of geomorphological importance. Statens Naturvårdsverk, PM 679, 80.

Melander, O., 1976. Geomorphological map 29G STIPOK, 29 H Sitasjaure och 30 H Riksgränsen (west): description and assessment of areas of geomorphological importance. Statens Naturvårdsverk, PM 733, 80.

Melander, O., 1982. Geomorphological map 28H Sarek Description and assessment of areas of geomorphological importance. Statens Naturvårdsverk, PM 1490, 58.

Møller, J.J., 1987. Shoreline relation and prehistoric settlement in northern Norway. Nor. J. Geogr. 41 (1), 45–60. https://doi.org/10.1080/00291958708552171.

Møller, J.J., 2003. Late quaternary sea level and coastal settlement in the european north. J. Coast. Res. 19 (3), 731–737. Retrieved from. http://www.jstor.org/stable/4299209.

Ottesen, D., Dowdeswell, J.A., 2006. Assemblages of submarine landforms produced by tidewater glaciers in Svalbard. J. Geophys. Res. 111, F01016. https://doi.org/10.1029/2005JF000330.

Patton, H., Hubbard, A., Andreassen, K., Auriac, A., Whitehouse, P.L., Stroeven, A.P., Shackleton, C., Winsborrow, M., Heyman, J., Hall, A.M., 2017. Deglaciation of the Eurasian ice sheet complex. Quat. Sci. Rev. 169, 148–172. https://doi.org/10.1016/j.quascirev.2017.05.019.

Pettersen, K., 1887. De geologiske bygningsforholde langs den nordlige side af Torne träsk. Geol. Foren. Stockh. Forh. 9 (6), 420–433. https://doi.org/10.1080/11035898709443575.

Rodhe, L., 1988. Glaciofluvial channels formed prior to the last deglaciation: examples from Swedish Lapland. Boreas 17 (4), 511–516. https://doi.org/10.1111/j.1502-3885.1988.tb00565.x.

Rosén, P., Segerström, U., Eriksson, L., Renberg, I., Birks, H.J.B., 2001. Holocene climatic change reconstructed from diatoms, chironomids, pollen and near-infrared spectroscopy at an alpine lake (Sjuodjijaure) in northern Sweden. Holocene 11 (5), 551–562. https://doi.org/10.1191/095968301680223503.

Rönnberg, A., 2011. Höjdmodellens noggrannhet. Lantmäteriet Informationsförsörjning, Lantmäteriet 1–7.

Sjögren, P., Damm, C., 2018. Holocene vegetation change in Northernmost Fennoscandia and the impact on Prehistoric Foragers 12 000–2000 Cal. A BP – A review. Boreas. https://doi.org/10.1111/bor.12344.

Stroeven, A.P., Hättestrand, C., Kleman, J., Heyman, J., Fabel, D., Fredin, O., Goodfellow, B.W., Harbor, J.M., Jansen, J.D., Olsen, L., Caffee, M.W., Fink, D., Lundqvist, J., Rosqvist, G.C., Stromberg, B., Jansson, K.N., 2016. Deglaciation of Fennoscandia. Quat. Sci. Rev. 147, 91–121. https://doi.org/10.1016/j.quascirev.

2015.09.016.
Svendsen, J.I., Mangerud, J., 1987. Late Weichselian and Holocene sea-level history for a cross-section of western Norway. J. Quat. Sci. 2 (2), 113–132. https://doi.org/10.1002/jqs.3390020205.
Svenonius, F., 1885. In: Minutes of Meeting 10 April 1885. Geologiska Föreningen I Stockholms Förhandlingar, vol. 7, pp. 605–609. https://doi.org/10.1080/11035898509444146.
Svenonius, F., 1886. Anmälanden och kritiker »Om seter eller strandlinjer i store höjder over havet.». Geol. Foren. Stockh. Forh. *8* (1), 55–57. https://doi.org/10.1080/11035898609442404.
Tsutaki, S., Nishimura, D., Yoshizawa, T., Sugiyama, S., 2011. Changes in glacier dynamics under the influence of proglacial lake formation in Rhonegletscher, Switzerland. Ann. Glaciol. *52* (58), 31–36. https://doi.org/10.3189/172756411797252194.
Tsutaki, S., Sugiyama, S., Nishimura, D., Funk, M., 2013. Acceleration and flotation of a glacier terminus during formation of a proglacial lake in Rhonegletscher, Switzerland. J. Glaciol. *59* (215), 559–570. https://doi.org/10.3189/2013JoG12J107.
Ulfstedt, A.C., 1977. Geomorphological maps 26 F Nasafjäll and 26 G Pieljekaise-description and assessment of areas of geomorphological importance. Statens Naturvårdsverk, PM *860*, 54.
Ulfstedt, A.C., 1979. Geomorphological map 27 G Sulitelma- Description and assessment of areas of geomorphological importance. Statens Naturvårdsverk, PM *1230*, 52.
Ulfstedt, A.C., 1980. Geomorphological maps 27H Kvikkjokk- Description and assessment of areas of geomorphological importance. Statens Naturvårdsverk, PM 1254, 58.